105 (2026) 106582

Contents lists available at ScienceDirect

Poultry Science

journal homepage: www.elsevier.com/locate/psj

Single-cell transcriptomics of chicken ovarian cancer identifying immune subsets with prognostic implications

Guoqiang Zhu [a,b,1], Susanna Chau Yi Wang [c,1], Hongqin Yao [a,b], Jiliang He [a,b], Jiannan Zhang [a,b], Mao Zhang [d], Yajun Wang [a,b,*]

[a] Key laboratory of Bio-resources and Eco-environment of Ministry of Education, College of Life Sciences, Sichuan University, Chengdu 610065, China
[b] Animal Disease Prevention and Food Safety Key Laboratory of Sichuan Province, College of Life Sciences, Sichuan University, Chengdu 610065, PR China
[c] University of New South Wales, School of Biological, Earth & Environmental Sciences, Sydney, 2052, Australia
[d] Division of Vascular Surgery, Sichuan Academy of Medical Sciences & Sichuan Provincial People's Hospital, School of Medicine, University of Electronic Science and Technology of China, Chengdu, 610072, China

ARTICLE INFO

Keywords:
Laying hen, Ovarian cancer model
Single-cell transcriptomics

ABSTRACT

Ovarian cancer (OC) is a lethal gynecological malignancy with a low 5-year survival rate. The lack of preclinical models accurately capturing OC's early pathogenesis contributes to this poor prognosis. The domestic laying hen uniquely develops spontaneous OC, but its single-cell-level insights for pathogenesis have been lacking. Here, we present the first single-cell transcriptomic atlas of ovarian tissues from 110-week-old laying hens with or without OC. We annotated 12 core cellular lineages and characterized tumor-associated changes, including increased CD4+ and CD8+ *T* cells and reduced macrophages in OC samples. T cells sub-clustering revealed conserved cell subtype-specific pH homeostasis regulation profiles across species. Notably, gene signatures from the two dominant Cyto_CD8+ subsets exhibited opposing prognostic roles when validated against human OC datasets (GSE18520, GSE26712, GSE49997). This study confirms the laying hen as a valuable OC model by demonstrating cross-species conservation in cellular heterogeneity and oncogenic pathways, advancing it from a pathologically analogous system to a molecularly traceable tool.

Introduction

Epithelial ovarian cancer remains the deadliest gynecological malignancy, with approximately 70% of patients diagnosed at advanced-stage metastatic disease and a 5-year survival rate below 30% (Malvezzi et al., 2016; Webb and Jordan, 2024). Current preclinical models do not fully recapitulate this disease pathogenesis (Tsang, et al., 2022). Genetically engineered mouse models, such as *MIS-RII-CRE*-driven strains, and the chemically induced rat models, rarely develop spontaneous ovarian tumors (Lengyel, et al., 2014). Although 3D in vitro models effectively dissect cell-autonomous mechanisms, they lack the systemic tumor microenvironment essential for studying metastasis (Bradaric, et al., 2013).

The domestic laying hens (*Gallus gallus domesticus*) serves as a valuable model for ovarian cancer research (Bernardo, et al., 2015; Barua and Bahr, 2022; Johnson and Giles, 2013). This unique non-human species spontaneously develops epithelial ovarian cancer, with age-dependent incidence rates of 24% in 3.5-year-old hens and up to 60% in 4-year-old hens (Johnson and Giles, 2006, 2013). Critically, its reproductive biology aligns with Fathalla's incessant ovulation hypothesis (Fathalla, 1971), mimicking the human reproductive risk profile through daily ovulation. Laying hen tumors recapitulate all major human histological subtypes, including serous, endometrioid, mucinous, and clear-cell carcinomas, and exhibit hallmark metastatic patterns such as intra-abdominal seeding and ascites accumulation (Barua, et al., 2009; Giles, et al., 2006;). This model enables investigation of early neoplastic events, such as preneoplastic dysplasia, which are inaccessible in humans (Barua, et al., 2009). Genetic strain differences in tumor susceptibility, such as the higher incidence observed in C strain compared to K strain among the laying hens, facilitate studies of heritable pathogenic mechanisms (Johnson and Giles, 2006).

The laying hen model offers significant translational value beyond elucidating carcinoma development mechanisms. Oral contraceptives demonstrate consistent protective effects across species. In humans, the

* Corresponding author.
E-mail address: cdwyjhk@163.com (Y. Wang).
[1] These authors are contributed equally to this work.

https://doi.org/10.1016/j.psj.2026.106582
Received 10 October 2025; Accepted 1 February 2026
Available online 2 February 2026

European Prospective Investigation into Cancer and Nutrition confirmed their risk-lowering association with ovarian cancer (Tsilidis, et al., 2011) and a collaborative reanalysis of 45 studies reported a 40-50% risk reduction (Cancer, 2008). In laying hens, progestin alone or with estrogen decreases ovarian cancer prevalence by 91% and 81% respectively (Treviño, et al., 2012). Curcumin exhibits cross-species efficacy, modulating human-relevant oncogenic pathways, such as *NF-κB* and *STAT3* inhibition, to reduce spontaneous ovarian cancer incidence by 57% in hens (Shi, et al., 2006; Sahin, et al., 2018). Flaxseed similarly aligns with human mechanisms, altering estrogen metabolism to promote 2-methoxyestradiol-induced apoptosis (Ansenberger, et al., 2010; Dikshit, et al., 2017; Fabová, et al., 2023; Keykhasalar, et al., 2021). Genistein also induces G2/M cell cycle arrest and apoptosis via DNA damage in humans (Gossner, et al., 2007; Lee, et al., 2012; Ouyang, et al., 2009), and reduces tumor incidence of 66.7% in hens by suppressing inflammatory cytokines and *GSK-3* signaling (Erten, et al., 2021; Sahin, et al., 2019). Nanoparticle delivery further enhances translational potential, with doxorubicin-loaded nanoparticles eliminating patient-derived tumors in hen chorioallantois membranes while reducing toxicity (Chu, et al., 2022; Vu, et al., 2018). These consistent cross-species responses validate the laying hen as a critical preclinical tool for ovarian cancer therapeutics development.

Advances in omics have significantly advanced ovarian cancer research. Microarray analyses identified oviduct-related genes enriched in tumors of GSE21706 (Treviño, et al., 2010), and flaxseed-modulated genes linked to chemoprevention in GSE40376 (Hales, et al., 2014). Our prior comparative transcriptomics between hens and women revealed 81 conserved pathways and 174 core genes across species in GSE246604, highlighting GPR37 as a novel prognostic and immunotherapy biomarker in ovarian cancer (Zhu, et al., 2024). However, bulk RNA-seq data inherently fails to resolve intra-tumoral cellular heterogeneity, meaning these bulk analyses cannot capture cell-type-specific alterations critical for deciphering ovarian tumor heterogeneity (Hales, et al., 2014; Treviño, et al., 2010; Zhu, et al., 2024). Consequently, single-cell analysis of chicken ovarian tissues is urgently needed. In this study, we performed single-cell RNA-seq on ovarian tissues from 110-week-old hens with and without ovarian cancer, and establish cross-species cellular heterogeneity and oncogenic pathway comparisons. This approach thereby enhances the translational value of the laying hen as an ovarian cancer model.

Materials and methods

Study design and animal sample acquisition

Six 110-week-old Lohmann Layer strain hens were obtained from Runfeng Poultry Cooperative in Sichuan Province, China, including three healthy hens and three with ovarian cancer. All procedures complied with China's Ministry of Science and Technology Guidelines for Experimental Animals and were approved by the Sichuan University Animal Ethics Committee with permission ID SCU2203012.

Hens were euthanized via cervical dislocation with immediate ovarian tissue dissection on ice. Ovarian cancer staging followed morphological criteria from our previous study (Zhu, et al., 2024). Healthy ovaries featured intact follicular hierarchy including large preovulatory follicles and ordered small follicles. Ovarian cancer tissues were defined by solid nodular outgrowths, marked ovarian volume shrinkage, absence of large preovulatory follicles, and/or ascites. All ovarian cancer samples were classified as late-stage per these criteria. (Zhu, et al., 2024). For single-cell RNA sequencing (scRNA-seq), three biological replicates each of healthy ovarian tissues and ovarian cancer tissues, were selected and immediately snap-frozen in liquid nitrogen. These samples were sent to SHBIO Biotechnology Co. Ltd. for processing using the DNBelab C series platform from BGI Genomics.

ScRNA-seq sample preparation and sequencing

Tissue dissociation and single-cell suspension preparation were conducted by BGI Genomics following their standardized protocol for fresh solid tissues using the DNBelab C series platform (Han, et al., 2022; Wang, et al., 2021a; Zhu, et al., 2023). Frozen tissues were thawed and minced into 1–2 mm^3 fragments, digested with collagenase IV and hyaluronidase at 37°C for 25 minutes, and filtered through 70 μm and 40 μm strainers to remove debris. Cells were resuspended in 1× phosphate-buffered saline with 0.04% BSA, and viability and concentration (600–1000 cells/μL) verified using a Countess II Automated Cell Counter (Invitrogen). scRNA-seq libraries were constructed using the BGI Single Cell Gene Expression Library Prep Kit (Senabouth, et al., 2020; Wang, et al., 2021b). Qualified single-cell suspensions were loaded onto a BGI Single Cell Chip to generate gel beads-in-emulsion for barcoded cDNA synthesis. Libraries were quantified using a Qubit 4.0 Fluorometer, then sequenced on an BGI500 platform.

Raw data preprocessing

Raw data preprocessing including quality control, adapter trimming and alignment, were performed by BGI Genomics. Low-quality reads were filtered with FastQC (Wingett and Andrews, 2018). Clean reads were aligned to the *Gallus gallus* reference genome using Hisat2 (Kim, et al., 2019). Cell-gene count matrices were generated with Htseq (Anders, et al., 2015). Sequencing data supporting this study have been deposited into CNSA (https://db.cngb.org/) with accession number CNP0008144.

Single-cell data quality control and normalization

Count matrices were imported into Seurat 4.4 for downstream analysis (Stuart, et al., 2019). Doublet detection was performed using the scDblFinder package to identify potential cell doublets (Germain, et al., 2022), which were excluded before quality control. Cells were filtered to remove low-quality populations, which defined those with fewer than 200 detected genes, more than 6000 detected genes, or more than 10% mitochondrial RNA were excluded (Stuart, et al., 2019). Qualified cells underwent normalized using LogNormalize, and 2000 highly variable genes were selected via variance stabilizing transformation (VST) for dimensionality reduction (Stuart, et al., 2019).

Cell clustering and annotation

Principal Component Analysis was performed using the selected highly variable genes, and the top 15 principal components (determined via elbow plot analysis) were used for Uniform Manifold Approximation and Projection (UMAP) visualization (Stuart, et al., 2019). Cells were clustered using the Louvain algorithm at resolution 0.2 via Seurat's FindClusters function (Stuart, et al., 2019).

Differential gene expression (DGE) analysis

Differential gene expression between healthy and ovarian cancer cell populations was identified using Seurat's FindMarkers function (Stuart, et al., 2019). Genes were considered differentially expressed if they met the criteria of adjusted $p < 0.05$ and absolute $\log_2$ fold change ($|\log_2 FC|$) > 0.25. Volcano plots illustrating DGE results were generated using the ggpubr package (Blighe, et al., 2019; Kassambara, 2018).

Pathway enrichment analysis

Gene Set Enrichment Analysis (GSEA) for KEGG pathways and Gene Ontology (GO) was performed using the clusterProfiler package [7]. Visualization of enrichment results was done with ggpubr (Kassambara, 2018).

T cell subclustering and annotation

T cells were subclustered from the integrated dataset using Seurat's Subset function, and re-clustered with the Louvain algorithm at resolution 0.8 to generate 16 distinct subclusters. Co-expression analysis of key marker genes was performed using Seurat's FeaturePlot function, with visualization at a color threshold of 0.2.

Cross-species clinical relevance analysis

Single-sample GSEA (ssGSEA) was performed using the GSVA (Hänzelmann, et al., 2013) to calculate enrichment scores of chicken Cyto_CD8$^+$_2 and Cyto_CD8$^+$_3 subcluster signatures in human ovarian cancer datasets (GSE18520, GSE27651, GSE49997). Patients were stratified into high- and low-score groups using the median score as the cutoff. Kaplan-Meier survival curves and log-rank tests were conducted with the survival and survminer packages to assess associations between signature scores and overall survival (Therneau and Lumley, 2015).

Statistical analysis

All statistical analyses were performed using R 4.2.2 with significance set at $p < 0.05$. Cell type/subcluster proportion differences between healthy and cancerous tissues were tested via Pearson's χ^2 test. DGE was determined using the MAST test (adjusted $p < 0.05$, $|\log_2 FC| > 0.25$) in Seurat (Stuart, et al., 2019). GSEA used 1000 permutations with clusterProfiler, with enriched terms defined by NES > 1.2 or < -1.2, $p < 0.05$. ssGSEA score comparisons between human tumor/normal tissues or high/low patient groups were done via Wilcoxon rank-sum test, and survival associations were evaluated with log-rank tests using the survival package (Hänzelmann, et al., 2013; Therneau and Lumley, 2015; Wu, et al., 2021). Multiple testing correction was performed using the Benjamini-Hochberg method.

Results

Single-cell transcriptional landscape of the chicken ovarian samples

To delineate cellular heterogeneity between healthy chicken ovaries and ovarian cancer samples, we first acquired fresh tissue samples, where the healthy ovaries exhibited well-organized follicular structures, whereas the ovarian cancer samples displayed disorganized tumor masses (Fig. 1A). After cell filtering, scRNA-seq yielded 23,412 cells from healthy ovaries designated as 110w_normal_ovary and 13,167 cells from ovarian cancer tissues designated as 110w_ovarian_cancer (Fig. 1B). UMAP dimensionality reduction revealed distinct clustering patterns between the two groups (Fig. 1B). Integrating all cells (n = 30,822), we annotated major cell lineages using canonical marker genes (Fig. 1C and 1D), including CD4$^+$ T cells (*CD3D, CD3E, CD4*), CD8$^+$ T cells (*CD3D, CD3E, CD8A*), B cells (*CD77B, PAX5, CD74*), plasma cells

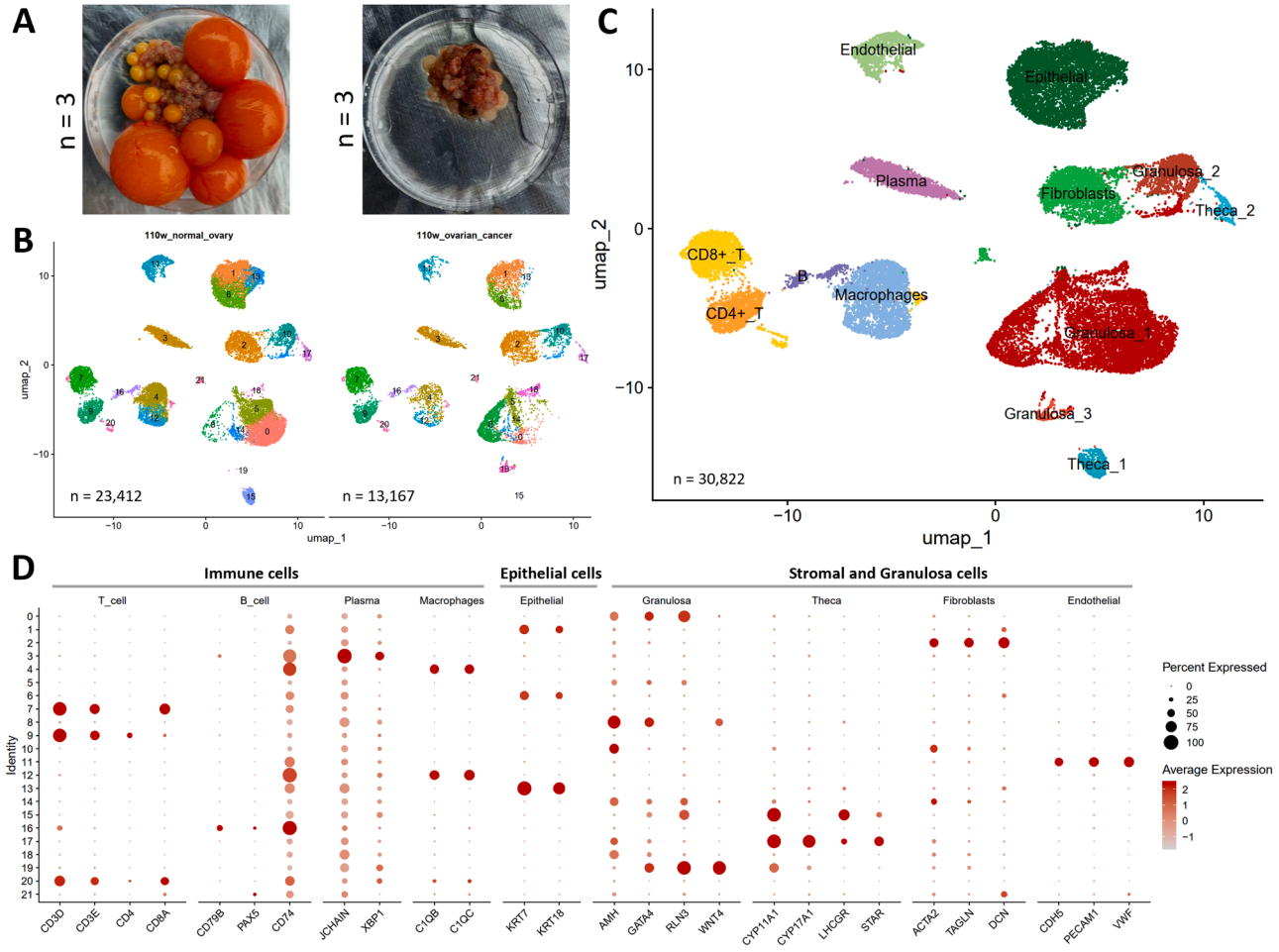

Fig. 1. Single-cell transcriptional profiling of healthy chicken ovaries and ovarian cancer samples. (A) Representative images of fresh tissue samples from 110-week-old healthy ovaries (left) and ovarian cancer samples (right). (B) UMAP plots showing cell clustering in healthy ovaries (left) and ovarian cancer samples (right). (C) UMAP plot of integrated cells annotated into major lineages: immune cells (CD8+ *T* cells, CD4+ *T* cells, B cells, plasma cells, macrophages), epithelial cells, and stromal & granulosa cells (granulosa cells, theca cells, fibroblasts, endothelial cells). (D) Dot plot validating lineage annotations via canonical marker genes; dot size denotes the percentage of cells expressing the gene, and color intensity represents average expression level.

(*JCHAIN, XBP1*), macrophages (*C1QB, C1QC*), epithelial cells (*KRT7, KRT18*), granulosa cells (*AMH, GATA4, RLN3, WNT4*), theca cells (*CYP11A1, CYP17A1, LHCGR, STAR*), fibroblasts (*ACTA2, TAGLN, DCN*), and endothelial cells (*CDH5, PECAM1, VMF*). Dot plots validated these annotations, with lineage-specific markers showing cell type-specific expression (Fig. 1D).

Immune cell remodeling in chicken ovarian cancer

Immune cells are a key component of the tumor microenvironment, and their dynamic remodeling directly regulates tumor progression and therapeutic responsiveness. UMAP visualization highlighted their distribution in healthy ovaries versus ovarian cancer samples (Fig. 2A). Quantitative analysis revealed significant immune subpopulation shifts, with ovarian cancer showing reduced macrophages but increased CD4+ and CD8+ *T* cells ($p = 4.17e\text{-}111$; Fig. 2B). Differential gene expression analyses uncovered distinct transcriptional profiles across immune subsets. CD8+ *T* cells exhibited 101 upregulated genes in ovarian cancer versus 61 in normal ovaries (Fig. 2C). $CD4^+$ T cells showed 57 upregulated genes in cancer versus 32 in healthy ovaries (Fig. 2D). Macrophages displayed 199 upregulated genes in cancer versus 83 in healthy ovaries (Fig. 2E). B cells had 18 upregulated genes in cancer versus 5 in healthy ovaries (Fig. 2F). Plasma cells exhibited 197 upregulated genes in cancer versus 54 in healthy ovaries (Fig. 2G). Total immune cells showed 646 upregulated genes in cancer versus 637 in healthy ovaries (Fig. 2H).

Non-immune cell remodeling in chicken ovarian cancer

Beyond immune cells, epithelial cells, stromal cells, and granulosa

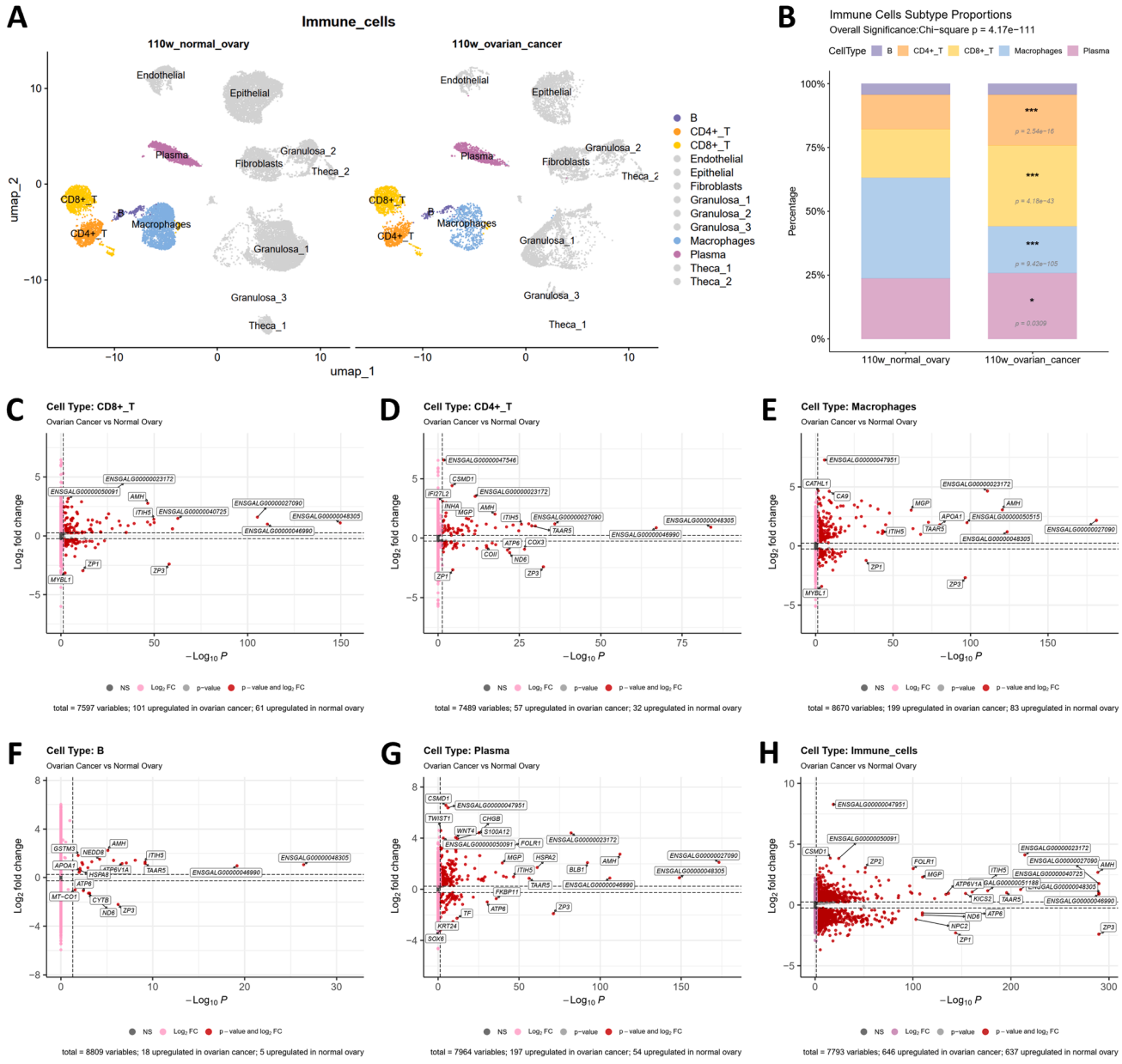

Fig. 2. Immune cell composition and transcriptional profiles in chicken ovarian cancer. (A) UMAP visualization highlighting immune cells in healthy ovaries (left) and ovarian cancer samples (right). (B) Stacked bar plots showing proportions of immune cell subtypes in healthy ovaries and ovarian cancer samples; overall significance was determined by Chi-square test. (C–H) Volcano plots of differential gene expression (DGE) for immune subsets: (C) CD8+ *T* cells, (D) CD4+ *T* cells, (E) macrophages, (F) B cells, (G) plasma cells, and (H) aggregated immune cells (ovarian cancer vs normal ovaries). Red dots indicate significantly upregulated genes, with labeled genes representing key differentially expressed transcripts.

cells also contribute to tumor progression within the tumor microenvironment. As shown in Fig. 3A and 3B, the epithelial cells exhibited extensive differential gene expression (DGE) in ovarian cancer, with 233 genes upregulated in ovarian cancer whereas 366 genes upregulated in normal ovaries. For stromal & granulosa cells (including granulosa, theca, fibroblasts, and endothelial cells; Fig. 3C), the DGE analysis revealed that endothelial cells had 45 genes upregulated in ovarian cancer while 167 genes upregulated in normal ovaries (Fig. 3D). The fibroblasts showed 93 genes upregulated in ovarian cancer and 129 genes upregulated in normal ovaries (Fig. 3E). As sown in Fig. 3F and 3G, the Granulosa_1 cells exhibited 3002 genes upregulated in ovarian cancer and 987 genes upregulated in normal ovaries. In contrast, the Granulosa_2 cells had 178 genes upregulated in ovarian cancer and 58 genes upregulated in normal ovaries. Theca_2 cells displayed 25 genes upregulated in ovarian cancer and 20 genes upregulated in normal ovaries (Fig. 3H).

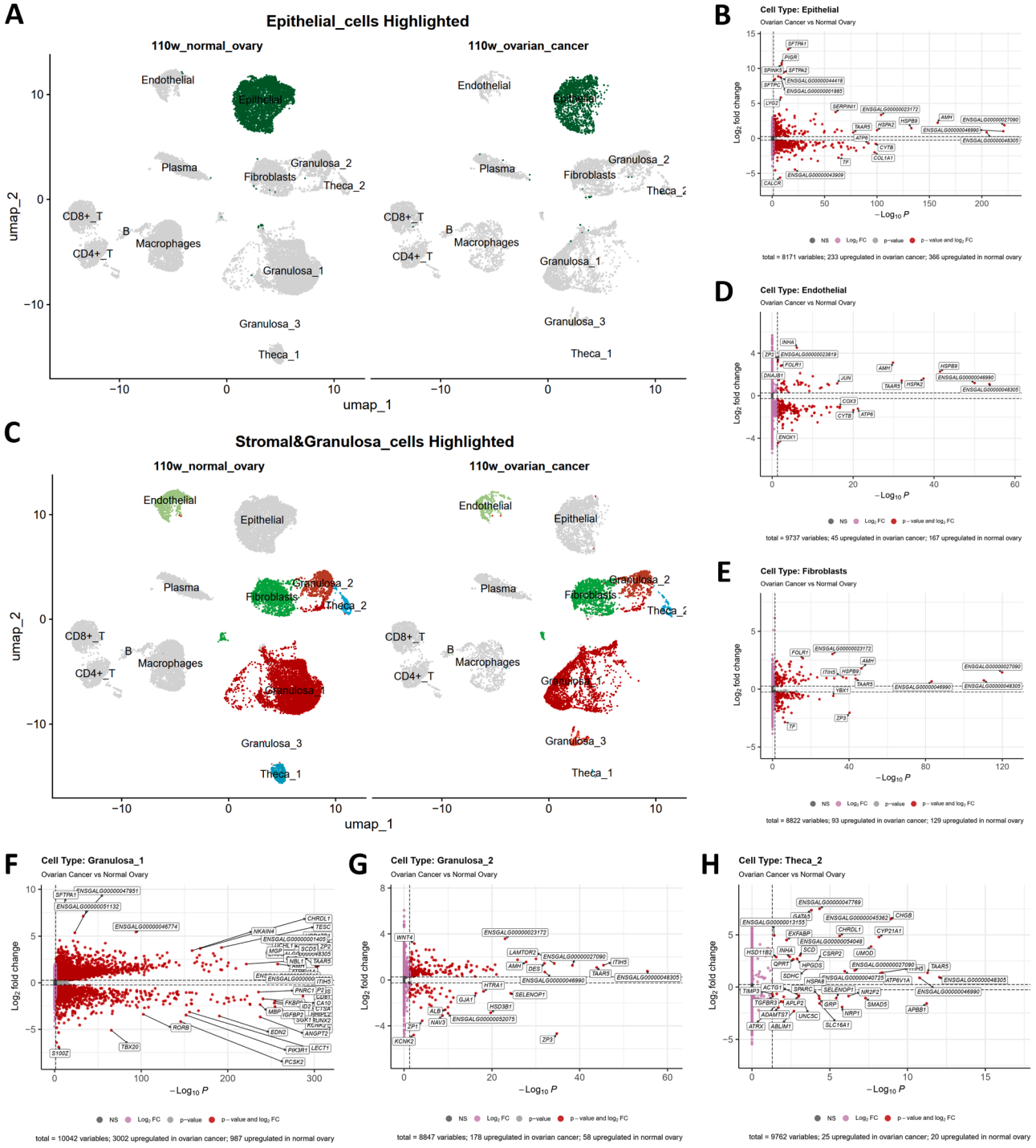

Fig. 3. Remodeling of epithelial and stromal cells in chicken ovarian cancer. (A) UMAP visualization highlighting epithelial cells in healthy ovaries (left) and ovarian cancer tissues (right). (B) Volcano plot of DGE for epithelial cells (ovarian cancer vs normal ovaries). (C) UMAP visualization highlighting stromal & granulosa cells (granulosa, theca, fibroblasts, endothelial cells) in healthy ovaries (left) and ovarian cancer tissues (right). (D–H) Volcano plots of DGE for stromal subsets: (D) endothelial cells, (E) fibroblasts, (F) Granulosa_1 cells, (G) Granulosa_2 cells, and (H) Theca_2 cells (ovarian cancer vs normal ovaries). Red dots indicate significantly upregulated genes, with labeled genes representing key differentially expressed transcripts.

Pathways enrichment in chicken ovarian cancer

To delineate cell-type-specific functional remodeling in ovarian carcinogenesis, we conducted the pathway enrichment analyses. The top-ranked pathways across different cell lineages were prioritized with the distinct top two GO pathways exhibited. As shown in Fig. 4A, the B cells showed the enrichment in cytoskeletal motor activity and signaling receptor regulator activity. The CD4+_T cells were enriched in regulation of GTPase activity and axon guidance. The CD8+_T cells displayed enrichment in chromosome, centromeric region and cell fate commitment. The Endothelial cells were enriched in cytosolic ribosome and nuclear chromosome. The Epithelial cells showed the enrichment in external encapsulating structure and steroid metabolic process. The fibroblasts were enriched in cell-cell adhesion mediator activity and modulation of chemical synaptic. The Granulosa_1 cells exhibited enrichment in DNA-binding transcription factor activity, RNA polymerase II-specific and transforming growth factor beta receptor superfamily signaling pathway. The Granulosa_2 cells were enriched in postsynaptic density and regulation of membrane potential. The Granulosa_3 cells showed enrichment in respiratory electron transport chain and structural constituent of ribosome. The Macrophages were enriched in cytokine activity and RNA helicase activity. The Plasma cells exhibited enrichment in organelle fusion and cell cycle process. Theca_1 cells were enriched in cytosolic small ribosomal subunit and sterol biosynthetic process. Theca_2 cells showed the enrichment in oxidative phosphorylation and iron ion binding.

Fig. 4. Cell type-specific functional pathway enrichment in chicken ovarian cancer. (A) Bar plot showing the top two Gene Ontology (GO) terms enriched for each cell type, with –log₁₀(qvalue) on the x-axis. (B–D) Enrichment plots of key pathways for immune subsets in ovarian cancer vs healthy ovaries: (B) CD4+ *T* cells, (C) CD8+ *T* cells, and (D) macrophages. The x-axis represents –log₁₀(qvalue), and bars indicate enriched pathways with labeled genes.

Given the critical role of immune cells in the tumor microenvironment, we further focused on CD4+ *T* cells, CD8+ *T* cells, and macrophages for further GSEA core enrichment analyses, where the most significant genes were listed. As shown in Fig. 4B, the CD4+_T cells showed the pathways enriched in cancer, including cell differentiation (*PLXNA2, RBPMS2, SIPA1, LAMA5, VDR, BEND6*), multicellular organism development, anatomical structure morphogenesis, neurogenesis, regulation of GTPase activity. In healthy ovaries, CD4+_T cells favored the pathways related to organelle lumen, nuclear lumen, ribosome biogenesis, rRNA processing and steroid biosynthetic process (*LBR, FDFT1, LSS, INIG1, SQLE, HSD17B7*). In CD8+_T cells, as shown in Fig. 4C, the cancer-enriched pathways included cellular developmental process, cell differentiation (*PCK2, MYL2, LAMA1, HEY2, RBPMS2, WNT4*), response to nutrient levels, ECM-receptor interaction, cell fate

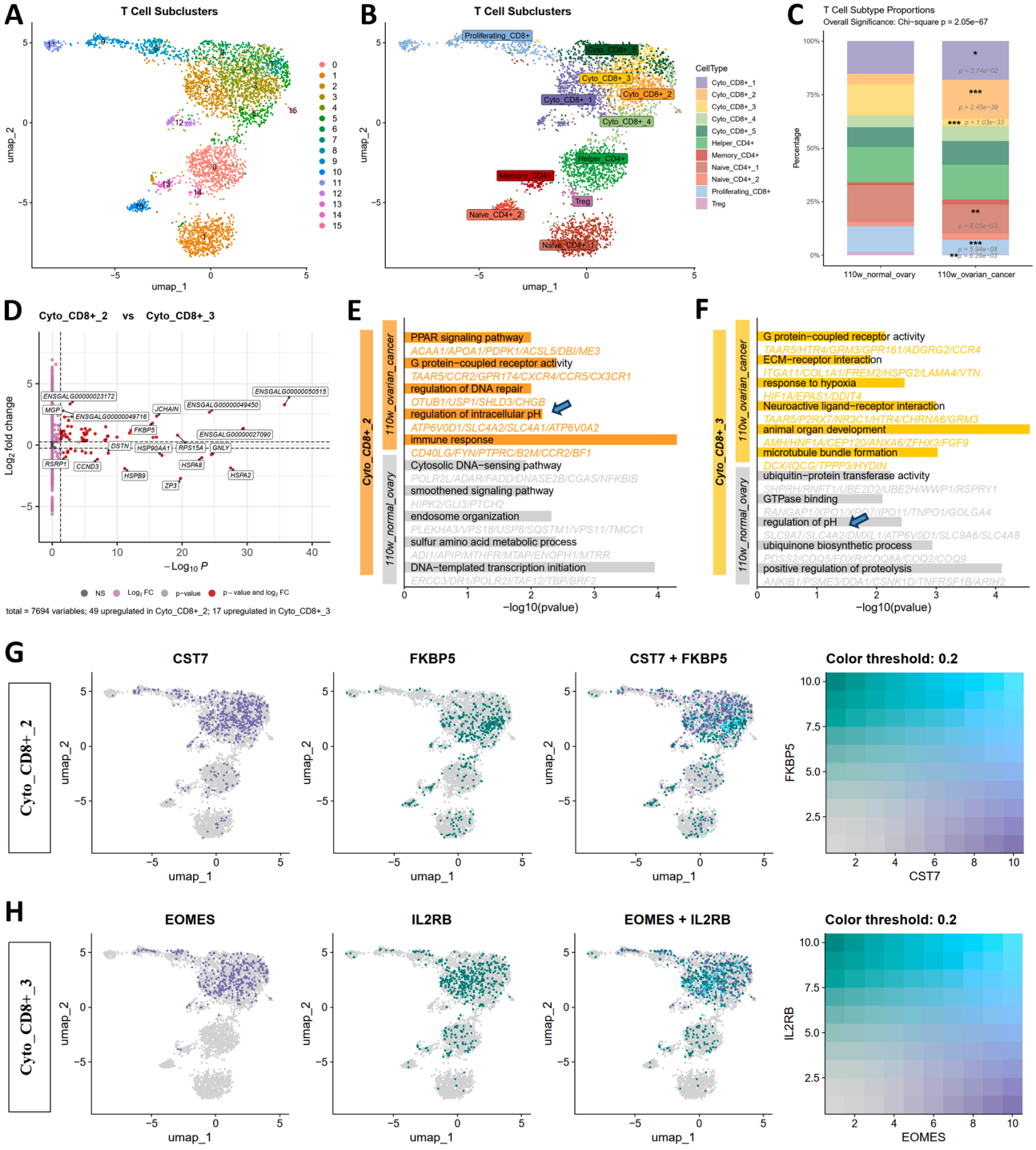

Fig. 5. Heterogeneity and functional specialization of T cell subclusters in chicken ovarian cancer. (A) UMAP plot showing 16 T cell subclusters identified by subclustering. (B) UMAP visualization annotating T cell subclusters by cell type and functional identity. (C) Stacked bar plots showing proportions of T cell subtypes in healthy ovaries and ovarian cancer samples; overall significance was determined by Chi-square test. (D) Volcano plot of differential gene expression between Cyto_CD8+_2 and Cyto_CD8+_3 subsets. (E, F) GSEA of pathways enriched in (E) Cyto_CD8+_2 and (F) Cyto_CD8+_3 subsets (ovarian cancer vs healthy ovaries). (G) UMAP plots showing co-expression of CST7 and FKBP5 in Cyto_CD8+_2. (H) UMAP plots showing co-expression of EOMES and IL2RB in Cyto_CD8+_3; color intensity in the rightmost panels represents combined expression level.

commitment, were revealed to be enriched in the ovarian cancer samples. In contrast, the CD8+_T cells from the healthy ovaries showed the enrichment in immune system process, myeloid leukocyte migration, sterol metabolic process (*HSD17B7, LBR, CYP11A1, MSMO1, INSIG1, DHCR7*) and cell cycle G2/M phase transition, steroid biosynthesis (*HSD17B7, LBR, DHCR24, CYP51A1, NSDHL, MSMO1*), chromosome segregation. In Macrophages, as shown in Fig. 4D, the cancer-enriched pathways including the G protein-coupled receptor signaling pathway (*ADGRA2, ACKR4, CX3CL1, IL8L1, ENDRA, SPNS2*), WNT signaling pathway (*WNT4, WNT6, ADGRA2, AXIN2, CTNNBIP1, TLE3*), growth factor binding, cytokine receptor activity, leukocyte chemotaxis, were enriched in chicken ovarian cancer samples. And the healthy ovarian macrophages were enriched in positive regulation of biosynthetic process, methyltransferase activity, membrane-enclosed lumen, monoatomic ion homeostasis, monoatomic ion homeostasis and RNA helicase activity.

T cell subclustering in chicken ovarian cancer

T cells serve as central effector cells mediating anti-tumor immune responses, and exhibit significant functional heterogeneity. To resolve this heterogeneity in ovarian carcinogenesis, we performed T cell subclustering, identifying 16 distinct subclusters visualized by UMAP (Fig. 5A). These subclusters were annotated by cell type and functional identity, including five cytotoxic CD8+ (Cyto_CD8+) subsets, proliferating CD8+, Helper CD4+, Memory CD4+, Naive CD4+, and regulatory T (Treg) lineages (Fig. 5B). Comparative analysis of T cell subtype proportions revealed statistically significant shifts between healthy ovaries and ovarian cancer tissues (overall Chi-square p = 2.05e-67). The Cyto_CD8+_2 and Cyto_CD8+_3 showed the most pronounced differences (P = 2.45e-39 and P = 1.03e-33, respectively) (Fig. 5C). Volcano plot analysis of Cyto_CD8+_2 versus Cyto_CD8+_3 identified 49 genes upregulated in Cyto_CD8+_2 cells and 17 genes upregulated in Cyto_CD8+_3 cells (Fig. 5D). For Cyto_CD8+_2 cells, the gene set enrichment analysis (GSEA, Fig. 5E) in ovarian cancer showed enriched pathways including PPAR signaling pathway (*ACAA1A, APOA1, PDPK1, ACSL5, DBI, ME3*), G protein-coupled receptor activity, regulation of DNA repair, regulation of intracellular pH (*ATP6V0D1, SLC4A2, SLC4A1, ATP6V0A2*), and immune response. Healthy ovary-derived Cyto_CD8$^+$_2 cells featured cytosolic DNA-sensing pathway, smoothened signaling pathway, endosome organization, sulfur amino acid metabolic process, and DNA-templated transcription initiation. For the Cyto_CD8+_3 cells, as shown in Fig. 5F, ovarian cancer enrichment included G protein-coupled receptor activity, ECM-receptor interaction, Neuroactive ligand-receptor interaction, animal organ development and microtubule bundle formation to be enriched. While healthy ovary enrichment involved ubiquitin-protein transferase activity, GTPase binding, regulation of pH (*SLC9A7, SLC4A2, DMXL1, ATP6V0D1, SLC9A6, SLC4A8*), ubiquitin biosynthetic process, positive regulation of proteolysis. UMAP-based gene co-expression mapping confirmed *CST7* and *FKBP5* as markers co-localizing specifically to Cyto_CD8+_2 (Fig. 5G), while *EOMES* and *IL2RB* co-localized to Cyto_CD8+_3 (Fig. 5H), validating these pairs as definitive identifiers for the two dominant cytotoxic CD8+ *T* cell subsets in ovarian carcinogenesis.

Clinical relevance of T cell subcluster signatures in chicken to human

To translate chicken ovarian cancer findings to humans, we applied single-sample gene set enrichment analysis (ssGSEA) to assess the signature enrichment of chicken Cyto_CD8+_2 and Cyto_CD8+_3 in human datasets (GSE18520, GSE26712, GSE49997). In GSE18520, Cyto_CD8$^+$_2 signature scores were significantly higher in human ovarian tumors than in normal tissues (p = 0.005), while Cyto_CD8$^+$_3 scores were elevated in normal tissues (p = 1.1e-05) (Fig. 6A). Similar patterns were observed in GSE26712, where the Cyto_CD8+_2 scores showed tumor enrichment (p = 0.025) and Cyto_CD8+_3 scores showed normal enrichment (p = 3.8e-07) (Fig. 6B). Subsequent survival analysis using GSE49997 demonstrated that low Cyto_CD8$^+$_2 scores correlated

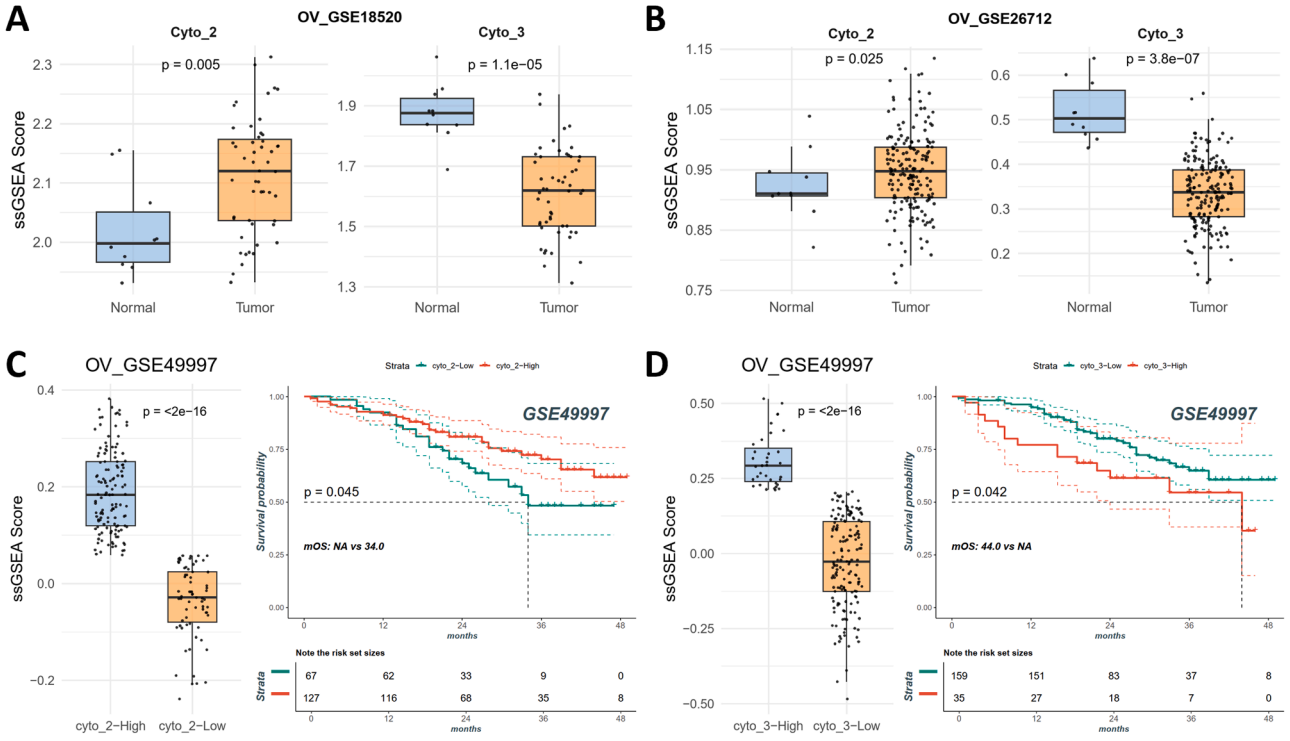

Fig. 6. Clinical relevance of T cell subcluster signatures in human ovarian cancer. (A, B) Single-sample gene set enrichment analysis (ssGSEA) scores for Cyto_CD8+_2 and Cyto_CD8+_3 signatures in human ovarian cancer datasets (GSE18520, GSE26712) comparing tumor vs normal tissues. (C, D) ssGSEA scores (left) and Kaplan–Meier survival curves (right) for Cyto_CD8+_2 (C) and Cyto_CD8+_3 (D) signatures in the GSE49997 dataset, stratified by high/low signature expression; log-rank test p-values and median survival (mOS) are indicated.

with poorer overall prognosis (Fig. 6C; log-rank $p = 0.045$), with a median survival time of 34.0 months versus not reached for low versus high groups (Fig. 6C). Conversely, high Cyto_CD8$^+$_3 scores (Fig. 6D) were associated with poorer prognosis (log-rank $p = 0.042$), showing a median survival time of 44.0 months versus not reached for high versus low groups. Significant differences confirmed conserved, opposing prognostic roles for these cytotoxic CD8$^+$ T cell subclusters in ovarian cancer.

Discussion

Molecular characterization of ovarian cancer mechanisms enables precision breeding for ovarian cancer-resistant chicken lines, directly reducing economic losses in poultry production. This study presents the first single-cell transcriptomic atlas of ovarian tissues from 110-week-old laying hens in both ovarian cancer and heathy groups (Johnson and Giles, 2013; Niebora, et al., 2024). We annotated 12 core cellular lineages encompassing immune, epithelial and stromal cells were annotated (Fig. 1C-D). Tumor-associated shifts included increased CD4+/CD8+ *T* cells and reduced macrophages, along with cell-type-specific transcriptional reprogramming were revealed. Our study identified 16 T cell subsets, revealing conserved pH homeostasis regulation in Cyto_CD8+ populations, and validated the opposing prognostic roles of Cyto_CD8+_2 and Cyto_CD8+_3 signatures in human ovarian cancer. This atlas provides a foundational framework for dissecting cell origins and heterogeneity in spontaneous ovarian tumors, advancing the laying hen from a pathologically analogous model to a molecularly traceable tool (Barua and Bahr, 2022; Niebora, et al., 2024).

Chicken ovarian cancer shows immune dynamics closely aligned with human ovarian cancer, validating the model's biological relevance. Chicken ovarian cancer exhibits increased CD4+ and CD8+ *T* cell proportions and decreased macrophages (Fig. 2B), mirroring the immune-infiltrated subtype observed in human ovarian cancer (Hornburg, et al., 2021; Yang, et al., 2024). Epithelial cells in chickens enrich extracellular matrix-related pathways (Fig. 4A), consistent with epithelial-mesenchymal transition in human ovarian cancer (Winterhoff, et al., 2017). Human single-cell studies identify similar epithelial-stromal heterogeneity (Winterhoff, et al., 2017), linking stromal cell states to tumor grade (Shih, et al., 2018). Recurrent immune subsets were characterized in both high-grade serous ovarian cancer (Gonzalez, et al., 2018). In chickens, granulosa cell subpopulations show extensive transcriptional reprogramming in tumors, with Granulosa_1 cells exhibiting 3,002 upregulated genes in ovarian cancer versus 987 in normal ovaries (Fig. 3F), echoing granulosa-like stromal remodeling in human ovarian cancer (Shih, et al., 2018). These parallels support the chicken model for ovarian cancer pathogenesis studies.

Present study validates the chicken model through conserved molecular pathways. Classic ovarian cancer biomarkers show cross-species consistency with CA125, a key human diagnostic marker, in spontaneous chicken ovarian adenocarcinomas and cultured chicken ovarian cancer cells (Jackson, et al., 2007). p53 mutations occur in 48% of chicken tumors, matching the high mutation rate in human cases (Hakim, et al., 2009). E-cadherin shows higher mRNA and protein expression in chicken cancerous ovaries versus normal tissues (Ansenberger, et al., 2009), consistent with its upregulation in human primary ovarian tumors (Ansenberger, et al., 2009). Aquaporin 5, which functions in water transport and cellular proliferation, shows abnormal expression in both chicken ovarian tumors and human ovarian cancer (Tiwari, et al., 2014; Yang, et al., 2006). We identified the conserved pH homeostasis regulation, a critical process for tumor cell survival and drug resistance (Sanhueza, et al., 2016; Webb, et al., 2011). Chicken Cyto_CD8+_2 cells in ovarian cancer enrich pH regulation pathways via genes including *ATP6V0D1, SLC4A2, SLC4A1,* and *ATP6V0A2* (Fig. 5E), while Cyto_CD8$^+$_3 cells in healthy ovaries utilize pH regulation genes such as *SLC9A7, SLC4A2, DMXL1, ATP6V0D1, SLC9A6,* and *SLC4A8* (Fig. 5F). This cancer-specific pH dysregulation aligns with human ovarian cancer mechanisms. The genes of pH regulation pathway were also mapped to the pathways with established roles in human ovarian cancer, where the *SLC4A* family members contributing to epithelial-stromal crosstalk in high-grade serous ovarian cancer (Gonzalez, et al., 2018; Qin, et al., 2017), and V-ATPase subunits like *ATP6V0A2* linking to serous ovarian cancer pathogenesis (Salvi, et al., 2022). Classic oncogenic pathways converge across species. *WNT* signaling, activated in chicken macrophages (Fig. 4D), links to human high-grade serous ovarian cancer initiation (Arend, et al., 2013; Teeuwssen and Fodde, 2019). T cell receptor signaling in chicken CD8+ *T* cells (Fig. 4C) mirrors its role as a hallmark of high T cell infiltration in human (Olalekan, et al., 2021). *NF-kB* and *STAT3* pathways, targeted by flaxseed to reduce chicken tumor incidence (Ansenberger, et al., 2010; Hales, et al., 2014), are well-characterized oncogenic pathways in human ovarian cancer (Stepień, et al., 2025). miR-200 family governs ovarian cancer spreading and serves as a blood biomarker in humans (Choi and Ng, 2017), with conserved functions and biomarker potential in chickens (Choi, et al., 2020a, 2020b). Cyclooxygenase expression dysregulation in chicken ovarian cancer (Hales, et al., 2008; Urick and Johnson, 2006), is consistent with its role in human disease (Daikoku, et al., 2005; Gupta et al., 2003).

Present study also confirms the translational relevance of chicken-derived cell subcluster signatures through cross-species ssGSEA. The chicken Cyto_CD8+_2 signature is enriched in human tumors, while the Cyto_CD8+_3 signature is enriched in normal human tissues (Fig. 5A, 5B). This pattern is consistent with the findings in human (Olbrecht, et al., 2021; Xu, et al., 2022). Survival analysis revealed their opposing prognostic roles, where the low Cyto_CD8+_2 scores or high Cyto_CD8+_3 scores correlate with poorer overall survival (Fig. 6C, 6D), aligning with T cell subpopulations dictating prognosis in human metastatic ovarian cancer (Deng, et al., 2022; Olalekan, et al., 2021). Ascites-related signatures also show cross-species relevance. Chicken ovarian cancer develops ascites (Barua, et al., 2009), and ascites-derived cell contribute to tumor progression and prognosis in humans (Chen, et al., 2023; Izar, et al., 2020; Zheng, et al., 2023). These findings validate the chicken model as a tool for translating basic discoveries to clinical applications.

In summary, we establish the first single-cell transcriptomic atlas of the ovarian tissues from110-week-old laying hens with or without ovarian cancer, filling a critical gap in spontaneous ovarian cancer model research. We identified 12 core lineages encompassing immune, epithelial and stromal cells. Tumor-associated shifts included increased CD4$^+$/CD8$^+$ T cells and reduced macrophages, along with lineage-specific transcriptional reprogramming. We further subclustered 16 T cell populations, uncovering conserved pH homeostasis regulation in Cyto_CD8+ populations, and validating opposing prognostic roles of Cyto_CD8+_2 and Cyto_CD8+_3 signatures in human ovarian cancer. The present study demonstrates the conserved cellular heterogeneity and oncogenic pathways across species, advancing the chicken ovarian cancer model from pathologically analogous to molecularly traceable. These findings provide insights into ovarian cancer microenvironment remodeling, identify potential prognostic markers, and bridge basic discoveries to clinical applications.

Supplementary material

All generated or analyzed data derived from our scRNA-seq has been included in this published article and CNSA (https://db.cngb.org/) with accession number CNP0008144. All data of this study are available from the corresponding author on reasonable request.

CRediT authorship contribution statement

Guoqiang Zhu: Writing – original draft, Visualization, Validation, Methodology, Formal analysis, Data curation, Conceptualization. **Susanna Chau Yi Wang:** Writing – original draft, Visualization, Software,

Methodology, Formal analysis, Data curation. **Hongqin Yao:** Validation, Methodology, Data curation. **Jiliang He:** Visualization, Validation, Software. **Jiannan Zhang:** Validation, Project administration, Funding acquisition. **Mao Zhang:** Writing – review & editing, Supervision, Project administration. **Yajun Wang:** Writing – review & editing, Writing – original draft, Validation, Supervision, Project administration, Funding acquisition, Conceptualization.

Disclosures

The authors declare that there are no conflicts of interest regarding the publication of this manuscript. The research was conducted in the absence of any commercial or financial relationships that could be construed as a potential conflict of interest.

Acknowledgments

This work was supported by grants from the Natural Science Foundation of Sichuan Province (2024NSFSC0299 and 2025ZNSFSC0282) and the Fundamental research funds for the central universities (SCU2025D003).

References

Anders, S., Pyl, P.T., Huber, W., 2015. HTSeq—A python framework to work with high-throughput sequencing data. Bioinformatics 31, 166–169.
Ansenberger, K., Richards, C., Zhuge, Y., Barua, A., Bahr, J.M., Luborsky, J.L., Hales, D. B., 2010. Decreased severity of ovarian cancer and increased survival in hens fed a flaxseed-enriched diet for 1 year. Gynecol. Oncol. 117, 341–347.
Ansenberger, K., Zhuge, Y., Lagman, J.A.J., Richards, C., Barua, A., Bahr, J.M., Hales, D. B., 2009. E-cadherin expression in ovarian cancer in the laying hen, Gallus domesticus, compared to human ovarian cancer. Gynecol. Oncol. 113, 362–369.
Arend, R.C., Londoño-Joshi, A..I., Straughn Jr, J.M., Buchsbaum, D.J., 2013. The wnt/β-catenin pathway in ovarian cancer: a review. Gynecol. Oncol. 131, 772–779.
Barua, A., Bahr, J.M., 2022. Ovarian cancer: applications of chickens to humans. Annu. Rev. Anim. Biosci. 10, 241–257.
Barua, A., Bitterman, P., Abramowicz, J.S., Dirks, A.L., Bahr, J.M., Hales, D.B., Bradaric, M.J., Edassery, S.L., Rotmensch, J., Luborsky, J.L., 2009. Histopathology of ovarian tumors in laying hens: a preclinical model of human ovarian cancer. Int. J. Gynecol. Cancer 19, 531–539.
Bernardo, A.D.M., Thorsteinsdottir, S., Mummery, C.L., 2015. Advantages of the avian model for human ovarian cancer. Mol. Clin. Oncol. 3, 1191–1198.
Blighe, K., S. Rana, and M. Lewis. 2019. EnhancedVolcano: publication-ready volcano plots with enhanced colouring and labeling. R package version 1:10.18129.
Bradaric, M.J., Penumatsa, K.., Barua, A., Edassery, S.L., Yu, Y., Abramowicz, J.S., Bahr, J.M., Luborsky, J.L., 2013. Immune cells in the normal ovary and spontaneous ovarian tumors in the laying hen (Gallus domesticus) model of human ovarian cancer. PLoS. One 8, e74147.
Cancer, C. G. o. E. S. o. O., 2008. Ovarian cancer and oral contraceptives: collaborative reanalysis of data from 45 epidemiological studies including 23 257 women with ovarian cancer and 87 303 controls. Lancet 371, 303–314.
Chen, W., Liu, H., Huang, X., Qian, L., Chen, L., Zhou, Y., Liu, Y., Liu, Y., Wang, Y., Zhang, T., 2023. A single-cell landscape of pre-and post-menopausal high-grade serous ovarian cancer ascites. iScience 26, 10.
Choi, P.-W., Bahrampour, A., Ng, S.-K., Liu, S.K., Qiu, W., Xie, F., Kuo, W.P., Kwong, J., Hales, K.H., Hales, D.B., 2020a. Characterization of miR-200 family members as blood biomarkers for human and laying hen ovarian cancer. Sci. Rep. 10, 20071.
Choi, P.-W., Ng, S.-W., 2017. The functions of microRNA-200 family in ovarian cancer: beyond epithelial-mesenchymal transition. Int. J. Mol. Sci. 18, 1207.
Choi, P.-W., So, W.W., Yang, J., Liu, S., Tong, K.K., Kwan, K.M., Kwok, J.S.-L., Tsui, S.K., Ng, S.-K., Hales, K.H., 2020b. MicroRNA-200 family governs ovarian inclusion cyst formation and mode of ovarian cancer spread. Oncogene 39, 4045–4060.
Chu, P.-Y., Koh, A.P.-F., Antony, J., Huang, R.Y.-J., 2022. Applications of the chick chorioallantoic membrane as an alternative model for cancer studies. Cells Tissues Org. 211, 222–237.
Daikoku, T., Wang, D., Tranguch, S., Morrow, J.D., Orsulic, S., DuBois, R.N., Dey, S.K., 2005. Cyclooxygenase-1 is a potential target for prevention and treatment of ovarian epithelial cancer. Cancer Res. 65, 3735–3744.
Deng, Y., Tan, Y., Zhou, D., Bai, Y., Cao, T., Zhong, C., Huang, W., Ou, Y., Guo, L., Liu, Q., 2022. Single-cell RNA-sequencing atlas reveals the tumor microenvironment of metastatic high-grade serous ovarian carcinoma. Front. Immunol. 13, 923194.
Dikshit, A., Hales, K., Hales, D.B., 2017. Whole flaxseed diet alters estrogen metabolism to promote 2-methoxtestradiol-induced apoptosis in hen ovarian cancer. J. Nutr. Biochem. 42, 117–125.
Erten, F., Yenice, E., Orhan, C., Er, B., ÖNER, P.D., Deeh, P.B.D., ŞAHİN, K., 2021. Genistein suppresses the inflammation and GSK-3 pathway in an animal model ofspontaneous ovarian cancer. Turk. J. Med. Sci. 51, 1465–1471.
Fabová, Z., Tarko, A., Mlynček, M., Kotwica, J., Sirotkin, A.V., 2023. Flaxseed can prevent adverse effects of toluene on human ovarian cell functions. Curr. Bioact. Compd. 19, 29–38.
Fathalla, M.F., 1971. Incessant ovulation—a factor in ovarian neoplasia? Lancet 298, 163.
Germain, P.-L., Lun, A., Meixide, C.G., Macnair, W., Robinson, M.D., 2022. Doublet identification in single-cell sequencing data using scDblFinder. f1000research 10, 979.
Giles, J.R., Olson, L..M., Johnson, P.A., 2006. Characterization of ovarian surface epithelial cells from the hen: a unique model for ovarian cancer. Exp. Biol. Med. 231, 1718–1725.
Gonzalez, V.D., Samusik, N.., Chen, T.J., Savig, E.S., Aghaeepour, N., Quigley, D.A., Huang, Y.-W., Giangarrà, V., Borowsky, A.D., Hubbard, N.E., 2018. Commonly occurring cell subsets in high-grade serous ovarian tumors identified by single-cell mass cytometry. Cell Rep. 22, 1875–1888.
Gossner, G., Choi, M., Tan, L., Fogoros, S., Griffith, K.A., Kuenker, M., Liu, J.R., 2007. Genistein-induced apoptosis and autophagocytosis in ovarian cancer cells. Gynecol. Oncol. 105, 23–30.
Gupta, R.A., Tejada, L..V., Tong, B.J., Das, S.K., Morrow, J.D., Dey, S.K., DuBois, R.N., 2003. Cyclooxygenase-1 is overexpressed and promotes angiogenic growth factor production in ovarian cancer. Cancer Res. 63, 906–911.
Hakim, A.A., Barry, C..P., Barnes, H.J., Anderson, K.E., Petitte, J., Whitaker, R., Lancaster, J.M., Wenham, R.M., Carver, D.K., Turbov, J., 2009. Ovarian adenocarcinomas in the laying hen and women share similar alterations in p53, ras, and HER-2/neu. Cancer Prev. Res. 2, 114–121.
Hales, D.B., Zhuge, Y.., Lagman, J.A.J., Ansenberger, K., Mahon, C., Barua, A., Luborsky, J.L., Bahr, J.M., 2008. Cyclooxygenases expression and distribution in the normal ovary and their role in ovarian cancer in the domestic hen (Gallus domesticus). Endocrine 33, 235–244.
Hales, K.H., Speckman, S..C., Kurrey, N.K., Hales, D.B., 2014. Uncovering molecular events associated with the chemosuppressive effects of flaxseed: a microarray analysis of the laying hen model of ovarian cancer. BMC Genom. 15, 709.
Han, L., Wei, X., Liu, C., Volpe, G., Zhuang, Z., Zou, X., Wang, Z., Pan, T., Yuan, Y., Zhang, X., 2022. Cell transcriptomic atlas of the non-human primate Macaca fascicularis. Nature 604, 723–731.
Hänzelmann, S., Castelo, R., Guinney, J., 2013. GSVA: gene set variation analysis for microarray and RNA-seq data. BMC Bioinform. 14, 7.
Hornburg, M., Desbois, M., Lu, S., Guan, Y., Lo, A.A., Kaufman, S., Elrod, A., Lotstein, A., DesRochers, T.M., Munoz-Rodriguez, J.L., 2021. Single-cell dissection of cellular components and interactions shaping the tumor immune phenotypes in ovarian cancer. Cancer Cell 39, 928–944.e926.
Izar, B., Tirosh, I., Stover, E.H., Wakiro, I., Cuoco, M.S., Alter, I., Rodman, C., Leeson, R., Su, M.-J., Shah, P., 2020. A single-cell landscape of high-grade serous ovarian cancer. Nat. Med. 26, 1271–1279.
Jackson, E., Anderson, K., Ashwell, C., Petitte, J., Mozdziak, P.E., 2007. CA125 expression in spontaneous ovarian adenocarcinomas from laying hens. Gynecol. Oncol. 104, 192–198.
Johnson, P., Giles, J., 2006. Use of genetic strains of chickens in studies of ovarian cancer. Poult. Sci. 85, 246–250.
Johnson, P.A., Giles, J.R., 2013. The hen as a model of ovarian cancer. Nat. Rev. Cancer 13, 432–436.
Kassambara, A. 2018. ggpubr:'ggplot2'based publication ready plots. R package version: 2.
Keykhasalar, R., Tabrizi, M.H., Ardalan, P., Khatamian, N., 2021. The apoptotic, cytotoxic, and antiangiogenic impact of Linum usitatissimum seed essential oil nanoemulsions on the human ovarian cancer cell line A2780. Nutr. Cancer 73, 2388–2396.
Kim, D., Paggi, J.M., Park, C., Bennett, C., Salzberg, S.L., 2019. Graph-based genome alignment and genotyping with HISAT2 and HISAT-genotype. Nat. Biotechnol. 37, 907–915.
Lee, J.-Y., Kim, H.S., Song, Y.-S., 2012. Genistein as a potential anticancer agent against ovarian cancer. J. Tradit. Complement. Med. 2, 96–104.
Lengyel, E., Burdette, J., Kenny, H., Matei, D., Pilrose, J., Haluska, P., Nephew, K., Hales, D., Stack, M., 2014. Epithelial ovarian cancer experimental models. Oncogene 33, 3619–3633.
Malvezzi, M., Carioli, G., Rodriguez, T., Negri, E., Vecchia, C.L.A, 2016. Global trends and predictions in ovarian cancer mortality. Ann. Oncol. 27, 2017–2025.
Niebora, J., Data, K., Domagała, D., Józkowiak, M., Barrett, S., Norizadeh Abbariki, T., Bryja, A., Kulus, M., Woźniak, S., Ziemak, H., 2024. Avian models for Human carcinogenesis—recent findings from molecular and clinical research. Cells 13, 1797.
Olalekan, S., Xie, B., Back, R., Eckart, H., Basu, A., 2021. Characterizing the tumor microenvironment of metastatic ovarian cancer by single-cell transcriptomics. Cell Rep. 35 (8), 109165.
Olbrecht, S., Busschaert, P., Qian, J., Vanderstichele, A., Loverix, L., Van Gorp, T., Van Nieuwenhuysen, E., Han, S., Van den Broeck, A., Coosemans, A., 2021. High-grade serous tubo-ovarian cancer refined with single-cell RNA sequencing: specific cell subtypes influence survival and determine molecular subtype classification. Genome Med. 13, 111.
Ouyang, G., Yao, L., Ruan, K., Song, G., Mao, Y., Bao, S., 2009. Genistein induces G2/M cell cycle arrest and apoptosis of human ovarian cancer cells via activation of DNA damage checkpoint pathways. Cell Biol. Int. 33, 1237–1244.
Qin, L., Li, T., Liu, Y., 2017. High SLC4A11 expression is an independent predictor for poor overall survival in grade 3/4 serous ovarian cancer. PLoS. One 12, e0187385.
Sahin, K., Orhan, C., Tuzcu, M., Sahin, N., Tastan, H., Özercan, İ.H., Güler, O., Kahraman, N., Kucuk, O., Ozpolat, B., 2018. Chemopreventive and antitumor

efficacy of curcumin in a spontaneously developing hen ovarian cancer model. Cancer Prev. Res. 11, 59–67.
Sahin, K., Yenice, E., Bilir, B., Orhan, C., Tuzcu, M., Sahin, N., Ozercan, I.H., Kabil, N., Ozpolat, B., Kucuk, O., 2019. Genistein prevents development of spontaneous ovarian cancer and inhibits tumor growth in hen model. Cancer Prev. Res. 12, 135–146.
Salvi, A., Young, A.N., Huntsman, A.C., Pergande, M.R., Korkmaz, M.A., Rathnayake, R. A., Mize, B.K., Kinghorn, A.D., Zhang, X., Ratia, K., 2022. PHY34 inhibits autophagy through V-ATPase V0A2 subunit inhibition and CAS/CSE1L nuclear cargo trafficking in high grade serous ovarian cancer. Cell Death. Dis. 13, 45.
Sanhueza, C., Araos, J., Naranjo, L., Villalobos, R., Westermeier, F., Salomon, C., Beltrán, A., Ramirez, M., Gutiérrez, J., Pardo, F., 2016. Modulation of intracellular pH in human ovarian cancer. Curr. Mol. Med. 16, 23–32.
Senabouth, A., Andersen, S., Shi, Q., Shi, L., Jiang, F., Zhang, W., Wing, K., Daniszewski, M., Lukowski, S.W., Hung, S.S., 2020. Comparative performance of the BGI and Illumina sequencing technology for single-cell RNA-sequencing. NAR Genom. Bioinform. 2, 34.
Shi, M., Cai, Q., Yao, L., Mao, Y., Ming, Y., Ouyang, G., 2006. Antiproliferation and apoptosis induced by curcumin in human ovarian cancer cells. Cell Biol. Int. 30, 221–226.
Shih, A.J., Menzin, A.., Whyte, J., Lovecchio, J., Liew, A., Khalili, H., Bhuiya, T., Gregersen, P.K., Lee, A.T., 2018. Identification of grade and origin specific cell populations in serous epithelial ovarian cancer by single cell RNA-seq. PLoS. One 13, e0206785.
Stepień, A.E., Trojniak, J.., Tabarkiewicz, J., 2025. Anti-oxidant and Anti-cancer properties of flaxseed. Int. J. Mol. Sci. 26, 1226.
Stuart, T., Butler, A., Hoffman, P., Hafemeister, C., Papalexi, E., Mauck, W.M., Hao, Y., Stoeckius, M., Smibert, P., Satija, R., 2019. Comprehensive integration of single-cell data. Cell 177, 1888–1902.e1821.
Teeuwssen, M., Fodde, R., 2019. Wnt signaling in ovarian cancer stemness, EMT, and therapy resistance. J. Clin. Med. 8, 1658.
Therneau, T.M., Lumley, T., 2015. Package 'survival'. R Top. Doc. 128, 28–33.
Tiwari, A., Hadley, J.A., Ramachandran, R., 2014. Aquaporin 5 expression is altered in ovarian tumors and ascites-derived ovarian tumor cells in the chicken model of ovarian tumor. J. Ovar. Res. 7, 99.
Treviño, L.S., Buckles, E..L., Johnson, P.A., 2012. Oral contraceptives decrease the prevalence of ovarian cancer in the hen. Cancer Prev. Res. 5, 343–349.
Treviño, L.S., Giles, J..R., Wang, W., Urick, M.E., Johnson, P.A., 2010. Gene expression profiling reveals differentially expressed genes in ovarian cancer of the hen: support for oviductal origin? Horm. Cancer 1, 177–186.
Tsang, S.I., Hassan, A..A., To, S.K., Wong, A.S., 2022. Experimental models for ovarian cancer research. Exp. Cell Res. 416, 113150.
Tsilidis, K., Allen, N., Key, T., Dossus, L., Lukanova, A., Bakken, K., Lund, E., Fournier, A., Overvad, K., Hansen, L., 2011. Oral contraceptive use and reproductive factors and risk of ovarian cancer in the European Prospective Investigation into Cancer and Nutrition. Br. J. Cancer 105, 1436–1442.
Urick, M., Johnson, P., 2006. Cyclooxygenase 1 and 2 mRNA and protein expression in the Gallus domesticus model of ovarian cancer. Gynecol. Oncol. 103, 673–678.
Vu, B.T., Shahin, S..A., Croissant, J., Fatieiev, Y., Matsumoto, K., Le-Hoang Doan, T., Yik, T., Simargi, S., Conteras, A., Ratliff, L., 2018. Chick chorioallantoic membrane assay as an in vivo model to study the effect of nanoparticle-based anticancer drugs in ovarian cancer. Sci. Rep. 8, 8524.
Wang, W., Zhong, Y., Zhuang, Z., Xie, J., Lu, Y., Huang, C., Sun, Y., Wu, L., Yin, J., Yu, H., 2021a. Multiregion single-cell sequencing reveals the transcriptional landscape of the immune microenvironment of colorectal cancer. Clin. Transl. Med. 11, e253.
Wang, X., He, Y., Zhang, Q., Ren, X., Zhang, Z., 2021b. Direct comparative analyses of 10X genomics chromium and smart-seq2. Genom. Proteom. Bioinform. 19, 253–266.
Webb, B.A., Chimenti, M.., Jacobson, M.P., Barber, D.L., 2011. Dysregulated pH: a perfect storm for cancer progression. Nat. Rev. Cancer 11, 671–677.
Webb, P.M., Jordan, S.J., 2024. Global epidemiology of epithelial ovarian cancer. Nat. Rev. Clin. Oncol. 21, 389–400.
Wingett, S.W., Andrews, S., 2018. FastQ screen: a tool for multi-genome mapping and quality control. F1000Research 7, 1338.
Winterhoff, B.J., Maile, M.., Mitra, A.K., Sebe, A., Bazzaro, M., Geller, M.A., Abrahante, J.E., Klein, M., Hellweg, R., Mullany, S.A., 2017. Single cell sequencing reveals heterogeneity within ovarian cancer epithelium and cancer associated stromal cells. Gynecol. Oncol. 144, 598–606.
Wu, T., Hu, E., Xu, S., Chen, M., Guo, P., Dai, Z., Feng, T., Zhou, L., Tang, W., Zhan, L., 2021. clusterProfiler 4.0: a universal enrichment tool for interpreting omics data. Innovation 2, 3.
Xu, J., Fang, Y., Chen, K., Li, S., Tang, S., Ren, Y., Cen, Y., Fei, W., Zhang, B., Shen, Y., 2022. Single-cell RNA sequencing reveals the tissue architecture in human high-grade serous ovarian cancer. Clin. Cancer Res. 28, 3590–3602.
Yang, J.-H., Shi, Y.-F., Cheng, Q., Deng, L., 2006. Expression and localization of aquaporin-5 in the epithelial ovarian tumors. Gynecol. Oncol. 100, 294–299.
Yang, W., Liu, S., Mao, M., Gong, Y., Li, X., Lei, T., Liu, C., Wu, S., Hu, Q., 2024. T-cell infiltration and its regulatory mechanisms in cancers: insights at single-cell resolution. J. Exp. Clin. Cancer Res. 43, 38.
Zheng, X., Wang, X., Cheng, X., Liu, Z., Yin, Y., Li, X., Huang, Z., Wang, Z., Guo, W., Ginhoux, F., 2023. Single-cell analyses implicate ascites in remodeling the ecosystems of primary and metastatic tumors in ovarian cancer. Nat. Cancer 4, 1138–1156.
Zhu, G., Wang, X., Wang, Y., Huang, T., Zhang, X., He, J., Shi, N., Chen, J., Zhang, J., Zhang, M., 2024. Comparative transcriptomic study on the ovarian cancer between chicken and human. Poult. Sci. 103, 104021.
Zhu, Q., Zhao, X., Zhang, Y., Li, Y., Liu, S., Han, J., Sun, Z., Wang, C., Deng, D., Wang, S., 2023. Single cell multi-omics reveal intra-cell-line heterogeneity across human cancer cell lines. Nat. Commun. 14, 8170.